will be published in **Astrophysical Bulletin, 2016, vol. 71, No. 1**

Detailed optical spectroscopy of the B[e] star MWC 17

V.G. Klochkova*, E.L. Chentsov

Special Astrophysical Observatory RAS, Nizhnij Arkhyz, 369167 Russia

November 25, 2015

Abstract Based on the data of multiple high-resolution R = 60000 observations obtained at the 6-m telescope (BTA) in combination with the Nasmyth Echelle Spectrograph (NES), we studied the features of the optical spectrum of the star MWC 17 with the B[e]-phenomenon. In the wavelength interval of 4050–6750 Å, we identied numerous permitted and forbidden emissions, interstellar Na I lines, and diffuse interstellar bands (DIBs). Radial velocities were estimated from lines of different origin. As the systemic velocity, Vsys, the velocity of the forbidden emissions can be accepted: −47 km/s (relative to the local standard Vlsr = −42 km/s). Comparison of the obtained data with the earlier measurements allows us to conclude on the absence of considerable variability of spectral details.

Key words. stars: emission-line, B[e]–stars: individual: MWC 17

arXiv:1511.07700v1 [astro-ph.SR] 24 Nov 2015

1. Introduction

The hot B-type star MWC 17 = V832 Cas is referred to the objects with the B[e] phenomenon [1, 2]. The B[e] phenomenon involves having a number of peculiar details in the stellar spectrum: primarily, strong emission lines of neutral hydrogen H I and helium He I, emissions of the permitted lines of metal ions, and low-excited forbidden lines. The second significant feature of stars with the B[e] phenomenon is large IR flux excess due to circumstellar hot dust. However, the stars which meet these two main criteria form a group of highly heterogeneous objects. Lamers et al. [3], having developed the classification criteria for the stars with the B[e]-phenomenon, divided them in five subtypes. They did not refer the star MWC 17 to any of those subtypes, it appears in publications as a member of the most populated B[e]-unclassified subgroup.

A few dozens of the unclassified stars with the B[e]-phenomenon were investigated by Miroshnichenko and coauthors. The review of the results obtained, including the spectral data from the 6-m telescope, is given in [4]. One of the results of the spectroscopic investigation lies in the fact that unclassified B[e]–stars are interacting binary systems in the broad range of luminosities. Objects with luminosities $L \leq 10^5 L_\odot$ are separated into a new group called the objects of the FS CMa type. About 30% of FS CMa type objects exhibit various signs of binarity. In [5], it is also suggested to consider the unclassified B[e]–stars as interacting binaries.

The main problem in the investigation of stars with the B[e] phenomenon is the estimation of stars luminosity. The luminosity would allow one to detect the evolution stage of the star and range it to one or another type of hot stars with similar features in the spectra. Still, in optical spectra of the stars with the B[e]-phenomenon, as a rule, one cannot find the absorptions which form in the stellar atmosphere conditions and could serve as criteria for luminosity estimation. The fact which also causes a problem is that two above mentioned distinctive features (spectral peculiarity and IR–flux excess) are intrinsic to several types of hot stars observed at the essentially different evolution stages: young

* E-mail: valenta@sao.ru

Herbig Ae/Be stars, evolved massive stars of high luminosity (LBV, supergiants), and far evolved low-mass stars which are close to the planetary nebula phase.

The situation with the B-type star VES 695, which is associated with the IR-source IRAS 00470+6429 and has an emission spectrum, properly illustrates the difficulties in determination of evolutionary status of stars with emission spectra. For a long time, this object had been considered as a possible protoplanetary nebulae (PPN) candidate at the stage close to the PN phase (see [6] and references therein). However, the complex study [7], carried out with a large volume of observation material, including the echelle spectra from the 6-m telescope, resulted in an alternate conclusion on the evolutionary status of VES 695. Complex of the obtained fundamental parameters (luminosity, characteristic features of energy distribution in the spectrum, binarity indications for the star) allowed Miroshnichenko et al. [7] to refer VES 695 to the stars of the FS CMa type.

MWC 17 which is associated with the IR-source IRAS 01441+6026 is one of the hottest stars with the B[e]-phenomenon. It is located near the galactic plane and has the coordinates: $\alpha(2000) = 01^h\,47^m\,38.5^s$, $\delta(2000) = +60^\circ\,41'\,57''$, $l = 129.8^\circ$, and $b = -1.4^\circ$. In the optical range, MWC 17 is quite a faint star with a magnitude $V = 11\overset{m}{.}7$ [8]. Due to high reddening, the star is weaker in the B band, $B = 13\overset{m}{.}5$ (according to the SIMBAD data), thus, its optical spectrum is understudied at present. Zickgraf [8] carried out the only spectroscopic study of MWC 17 with high spectral resolution. The spectral resolution of his data (R from 23000 to 45000) is comparable to ours, but this author used only small regions of the spectrum. The Hα, HeI 5876, [NII] 6583, [OI] 6300, [SIII] 6312, and [FeII] 7155 Å profiles are presented in [8] graphically. Relative intensities and radial velocities are given for these lines as well as for HeI 6678 and NaI 5890, 5896 Å.

To search for possible variability of the MWC 17 optical spectrum and to add data on its peculiarities, we made detailed identification and necessary measurements of the parameters of spectral details of different origin from the spectra obtained with a resolution R = 60000 in the broad wavelength range 4050–6750 Å. The observation data used is briefly described in Section 2. Section 3 presents information on the profile of spectral details found with the high-resolution spectra, their analysis, and discussion of the results derived. In Section 4, we deal with the position of MWC 17 in the Galaxy, and the main conclusions are summed up in Section 5.

2. Observed data

We use the MWC 17 spectra obtained on the 6-m telescope with the Nasmyth Echelle Spectrograph (NES) [9]. The spectrograph equipped with a CCD of 2048×2048 elements and an image slicer [10] provides R = 60000 in the wavelength range of 3500–6800 Å. One-dimensional spectra were extracted from two–dimensional echelle images using the modified [11] MIDAS Echelle context. Table 1 shows the dates of obtaining the spectra and the detected spectral intervals. Correction and control of instrumental coordination of spectra of the star and the lamp with a hollow cathode were fulfilled with the telluric lines [OI], O_2, and H_2O. The procedure of radial velocity Vr determination from the spectra obtained with NES and error sources are described in more detail in [12]. The root-mean-square error of the measurements is Vr≤0.8 km/s for single narrow line.

Table 1. Dates of obtaining the spectra used and the detected spectral interval

Date	$\Delta\lambda$, Å
15.11.2005	5275÷6735
15.01.2006	4570÷5980
16.01.2006	4570÷5980
14.03.2006	4050÷5450
02.09.2006	5275÷6735

3. Main types of line profiles

As early as in the first publication, when were mentioned some features of the MWC 17 spectrum [13], a remarkably high intensity of emissions was noted. Intensity variations, from peaks of the strongest HI, [OI] emissions to the NaI absorption cores, and therefore lowering of the signal-to-noise ratio, attain three orders of magnitude in the MWC 17 spectrum! Weak emissions, which are hardly distinguishable from noise, make it difficult to generate the continuum. Absorptions, by contrast, (except for depressions in the emission lines) are presented by the interstellar NaI (1) lines, the strongest of DIBs and, possibly, by the Hδ photospheric wings. With regard to these circumstances, we detected only small variations of the intensities of the lines and profile shapes and positions with time. The strongest emissions were on September 2, 2006; the residual intensities of the emission peaks in this spectrum are on the average 20% higher than in January and 30% higher than in March of the same year.

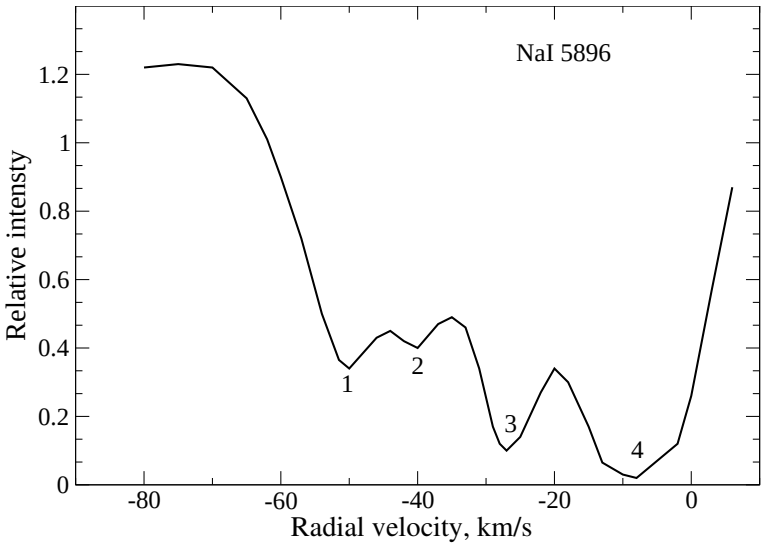

Figure 1. Profile of the NaI 5896 Å line in the spectrum of MWC 17 averaged over all available spectra. Numbers 1–4 denote the positions of four profile components from Table 3.

Heliocentric radial velocities, Vr, were found for the profiles on the whole or for separate details by coincidence of their direct and mirror images. When comparing Vr for the same lines in the spectra obtained on different dates, it should be taken into account that apart from random errors, systematic errors of the order of 1 km/s are also possible. Table 2 shows the examples of the comparison of our data with each other and with the data from [8]. The profile shape which is complex and changing from line to line does not allow us to confine ourselves to intensity and a single value of radial velocity only. These and additional profile parameters are collected in Tables 2, 3, 4, and 5. In these tables, r is the residual intensity of an emission peak or an absorption core, V/R is the ratio of residual intensities of the blue and red components for double–peaked emissions. The velocities are rounded to whole km/s, they correspond to:

Vr – the upper part of the whole profile for the emission or the lower part of the absorption component;

V_{em} – the emission peaks of a double-peaked profile;

V_{abs} – the depression in the upper part of the emission line profile;

V(r/2) – the shortwave and longwave (hereinafter "blue" and "red") slopes of the emission line profile at the half maximum intensity;

V(r≈1) – the blue and red boundaries of the emission at the bottom of the profile.

The results from [8] are given in italics. Table 3 gives the velocities measured from the NaI (1) absorption components.

As follows from Table 2, the variations of radial velocities for strong emissions [OI] with distinct profiles in our two spectra, and the discrepancy with the data from [8] do not go beyond the mea-

Table 2. Profile parameters (see in the text) for some lines and dates according to our measurements and Zickgraf` s data [8] (in italics). Heliocentric velocities Vr are in km/s. Uncertain measurements are marked with a colon

Date	r	V/R	Vr	V_{em}		V_{abs}	V(r/2)		V(r≈1)	
[OI] 6300										
15.11.05	33	0.94	−48	−59	−38	−51	−74	−23	−92	0
2.09.06	33	0.97	−48	−57	−40	−49	−75	−24	−95	−5
	25	*0.91*	*−47:*	*−59*	*−39*	*−51*	*−72:*	*−21:*	*−92:*	*−2:*
[FeII] 5334										
15.11.05	3.7		−48				−72	−26	−95:	3:
15.01.06	3.7		−46				−71	−24	−94:	−1:
16.01.06	4.2		−47				−72	−23:	−95:	0:
14.03.06	3.7		−46				−72	−26:	−93:	−5:
02.09.06	4.9		−47				−72	−28	−94:	−5:
[NII] 5755										
15.11.05	16	0.84	−47	−65	−32	−52	−85:	−16	−125:	5
15.01.06	14	0.82	−47	−64	−31	−53	−86:	−15	−125:	6
16.01.06	15	0.80	−47	−64	−32	−55	−85:	−15:	−124:	10:
02.09.06	21	0.80	−48	−64:	−32	−52	−83:	−17	−120:	7:
FeII 5169										
15.01.06	5.7	0.74	−42	−55:	−36	−50:	−69:	−16	−98:	2:
16.01.06	6.7	0.72	−41	−55:	−37	−51:	−71:	−18	−102:	0:
14.03.06	4.6	0.78	−43	−57:	−35	−51:	−71:	−19:	−97:	5:
FeII 5316										
15.11.05	13	1.00	−51	−69	−35	−50	−88	−13	−112	11
15.01.06	11	0.95	−51	−68	−37	−51	−88	−14	−115:	12:
16.01.06	12	0.94	−51	−69	−36	−52	−88	−14:	−111:	14:
14.03.06	10	1.07	−52	−70	−33	−52:	−90:	−13:	−115:	14:
02.09.06	15	1.12	−54	−70	−34	−49	−90	−15	−108:	11
FeII 6318										
15.11.05	8.5	0.94	−50		−34	−50	−86	−13	−105:	8:
02.09.06	9.1		−53		−39		−89	−15	−105:	8:
[SIII] 6312										
15.11.05	4.0	0.73	−47:		−25		−81:	−12	−118:	10:
02.09.06	5.3	0.68	−46:	−66:	−28	−50	−80:	−14	−122:	6:
	3.1	*0.76*	*−50:*	*−70*	*−25*	*−44*	*−88:*	*−12:*	*−123:*	*4:*
HeI 5876										
15.11.05	7	0.82	−54	−78 :	−28	−52:	−108	−6	−145:	25
15.01.06	6	0.76	−50	−70:	−27	−57:	−110	−3	−142:	33:
16.01.06	6	0.75	−48:		−26		−106:	−3:	−150:	33
02.09.06	9	0.75	−56	−80:	−33		−110	−11	−140:	20:
	6	*0.68*	*−50:*	*−78*	*−24*	*−57*	*−105:*	*0:*	*−135:*	*30:*
HeI 6678										
15.11.05	2.3	0.84	−51	−72	−23	−60:	−106:	−1 :	−138:	20:
02.09.06	2.7	0.78	−54:		−28:		−105:	−2 :	−135:	22:
				−67	*−20*	*−53*				
Hα										
15.11.05				−105:	−10	−54				
02.09.06				−100:	−13	−55				
				−101	*−11*	*−59*				

surement error. The same can be said about the weaker [NII] and [FeII] emissions. Velocity variations from spectrum to spectrum for other lines are notable. They are mainly due to the variations in the red regions of the profiles (the shifts of their red slopes and peaks). The shifts for the [SIII] and FeII emissions are about 2–3 km/s, for HeI 5876 Å they attain 5 km/s.

Red regions are also most variable in the complex absorption/emission profiles of the NaI doublet. Figure 1 shows the result of averaging the profiles of the NaI 5896 Å line using several our spectra. The emission component is presented in this figure only by its blue region (Vr of −60 km/s), its red region is overlapped by interstellar extinction. Table 3 shows that three blue components of the NaI 5896 Å line keep their positions while the red component is shifted on November 15, 2005 by −(5–6) km/s relative to its position in 2006.

The double-peaked Hα emission profile is of type III according to the Beals classification [14]. The position of emission peaks Vr≈ −100 and −12 km/s as well as the position of the absorption Vr≈ −55 km/s are almost constant both in our two spectra of 2005, 2006 and in the earlier spectrum by Zickgraf [8]. One can see the change in the strongest emission intensities as compared with the data from [8] (see Table A1 in that paper). Both the [OI] 6300 Å and [SIII] 6312 Å lines with an excitation potential of 3.3 eV are 30% stronger in our spectrum than those in [8]. The HeI 5876 Å line has scarcely varied as compared with the measurements by Zickgraf [8].

Table 3. Radial velocities Vr measured for the components of the NaI doublet D-lines for certain dates. Zickgrafs measurements are given in italics [8]

	Vr, km/s			
	1	2	3	4
NaI 5890				
15.11.2005	−52	−40	−25	−14
15.01.2006	−50	−38	−27	−8
16.01.2006	−50	−38	−27	−9
02.09.2006	−50	−38	−28	−9
	−52	*−41*	*−25*	*−13*
NaI 5896				
15.11.05	−50	−40	−25	−12
15.01.06	−50	−40	−27	−9
16.01.06	−50	−41	−27	−8
02.09.06	−53	−42	−26	−9
	−49	*−42*	*−25*	*−11*

Table 4 and Fig. 2 illustrate the hierarchy of emission profiles by width and degree of asymmetry: both increase from top lines of the table to the bottom. The velocities in this table are averaged for the groups of lines with a similar profile shape. They can be useful not only in estimating the structure and kinematics of the MWC 17 envelope but also in controlling the line identification accuracy. As mentioned in previous studies of MWC 17 (and which is commonly characteristic of B[e]–stars), the narrowest lines in the optical spectrum are the forbidden emissions [FeII] and [OI]. Both are almost symmetrical. The former ones have sharper peaks (bifurcation is notable only in some lines and in some our spectra), the latter ones have more distinctly forked peaks. The red peak of the [OI] profile is stronger than the blue one.

In accordance with the results from [8], such a ratio of peak intensities is amplified for the HI, HeI, and [SIII] lines. According to our data, it is also typical of [NII], [OIII], [FeIII] and generally of most emissions. An exception is provided by the FeII lines of low excitation (e.g., FeII (49, 48) 5316 Å, see Table 2), the blue component of which can be stronger than the red one.

The permitted FeII emissions are notably broader than the forbidden ones, and they are slightly asymmetric: the blue slope is steeper than the red one. The low and high-excitation FeII lines (about 3 and 10 eV respectively) noticeably differ by the shape of the profile upper part: it is close to rectangular for the latter ones (e.g., the FeII 6318 Å line proles in Table 2), the central depression is not distinct. Difference in widths of the permitted and forbidden emissions indicate that these groups of lines origin in different physical conditions.

The members of the 42-nd FeII multiplet, which is the strongest in the visible spectrum, stand out for their profile shape. They are as broad as the other FeII emissions but abruptly get narrow toward the tops due to intensity decrease in the blue half of the line. As can be seen from Table 4 and Fig. 2,

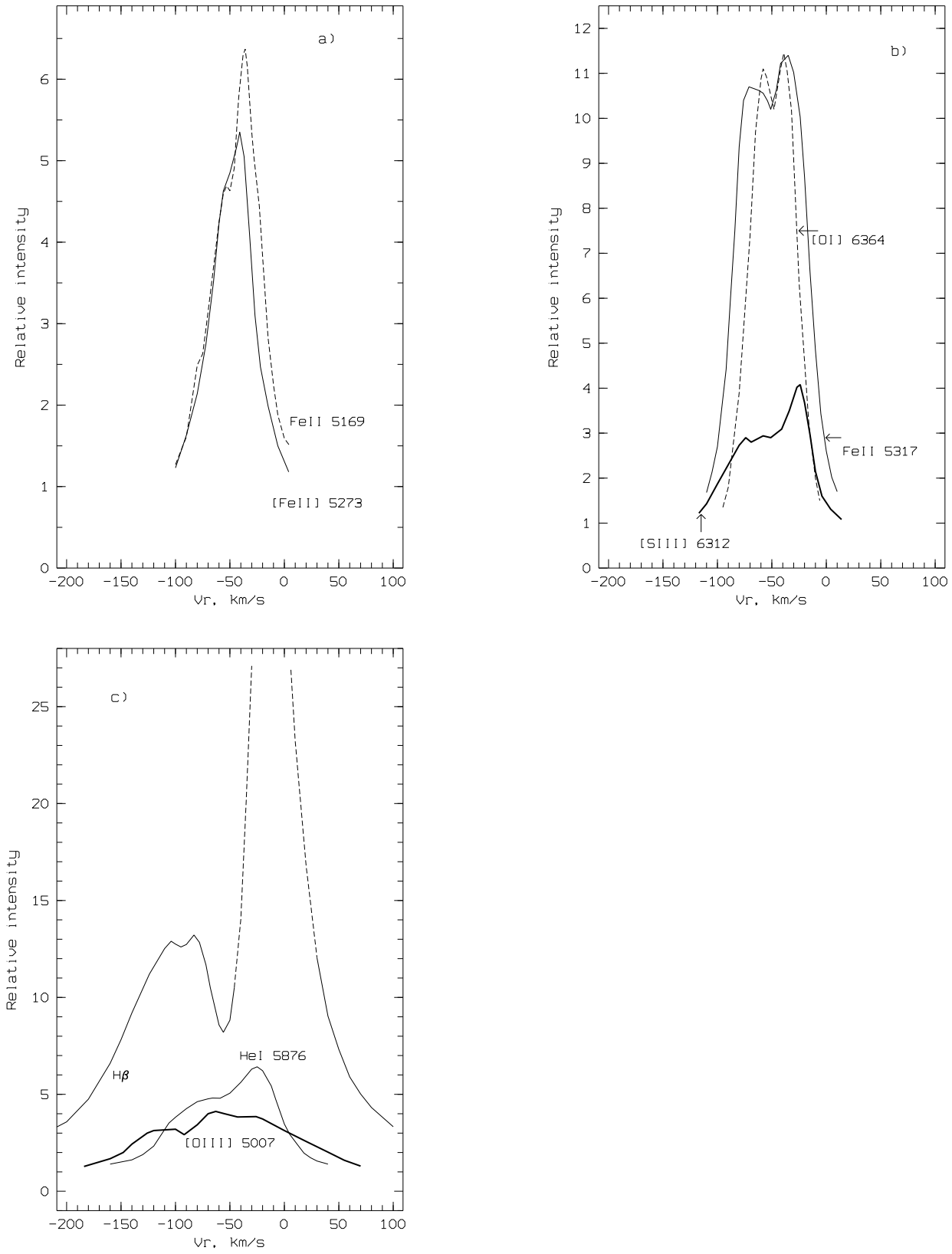

Figure 2. Profiles of the representative lines in the MWC 17 spectrum: (a) FeII 5169 Å (dashed line) and [FeII] 5273 Å (solid); (b) FeII 5317 Å (thin solid line), [SIII] 6312 Å (thick solid), and [OI] 6364 Å (dashed); (c) [OIII] 5007 Å (thick solid line), HeI 5876 Å (thin solid), and Hβ (thin solid, prolonged with the dashed line at high intensities).

the positions of the red emission peak and the whole red slope of the profile are almost the same as in other Fe II lines; the blue peak is weak and shifted toward the red region, it is faintly visible on the blue slope which is much smoother than the red one. Such asymmetry (the blue peak is not distinct and is weaker than the red one, the blue slope is smoother than the red one) is as well characteristic of emissions of forbidden ions [NII], [SIII], and [FeIII] which are broader at the bottom. It also remains in the broadest (exclusive of those of hydrogen) HeI and [OIII] lines. Among the model profiles [8], those are the most similar to the observed spectrum of MWC 17 which are computed for a tilted disk (i$\approx 45^\circ$), while Zickgraf [8] considers that i$\approx 80^\circ$ for MWC 17.

Table 4. Mean heliocentric radial velocities for emission groups in the MWC 17 spectrum with a similar profile shape. Designations are the same as for Table 2. Uncertain measurements are marked with a colon

Line type	Vr	V_{em}		V_{abs}	V(r/2)		V(r≈1)	
[FeII]	−47	−53:	−42:	−50	−72	−26	−95	−5:
[OI], [SII]	−48	−58	−39	−50	−74	−24	−93	−4
FeII low exc.	−51	−71	−34	−49	−89	−11	−105:	9
FeII high exc.	−51	−63:	−36:	−49:	−87	−14	−105:	9:
FeII(42)	−42	−55:	−36	−50:	−70	−18	−103:	5:
[NII], [SIII]	−47	−64	−30	−52	−83	−15	−120:	8:
HeI	−53 :	−76:	−28:	−55:	−108:	−6:	−142:	25:
[OIII]	−55 :	−100:	−50:	−78:	−130:	20:	−180:	90:
Hα, Hβ	−52 :	−95:	−12	−55				

Table 5 shows the identified lines and their parameters. As the discrepancies in the parameters from spectrum to spectrum for most lines are small, each line is presented here by a single set of the parameters. In the wavelength interval 4050–4570 Å, the parameters were obtained from the spectrum of March 14, 2006; in longer wavelength intervals, they were found by averaging two or more spectra. As follows from Table 5, we have not detected any absorptions in the MWC 17 spectrum with all the high-quality material in the broad wavelength interval. Using spectra with a resolution limit of 1.3 Å, Jaschek and Andrillat [15] found several absorptions forming in the stellar atmosphere: AlII 6066, SII 6102, NII 6632, and CII 6800 Å. We have not detected the rst three absorptions, which could occur in our spectral interval.

4. Location of MWC 17 in the Galaxy

If not particularly the radial velocity of the star itself (it may be peculiar), then at least the presence of the blue-shifted components in the interstellar NaI (1) lines with velocities of up to −50 km/s (there is even a weak component with a velocity of about −60 km/s) says that MWC 17 is located in the Perseus Arm or behind it. The distance to MWC 17 can be estimated by different methods, but the peculiarity of the object make all them unreliable.

– Spectrophotometric parallax. The absence of photospheric absorptions in the stars spectrum makes the accepted $(B\text{-}V)_0$ color index uncertain. Martel and Gravina [16] give the following for MWC 17: $V = 11\overset{m}{.}66$, $(B\text{-}V) = 0\overset{m}{.}42$; along with this, for early subtype B we obtain the color excess $E(B\text{-}V) \approx 0\overset{m}{.}65$ and visual brightness extinction $Av \approx 2\overset{m}{.}5$. Let us notice that we obtain a smaller excess $E(B\text{-}V) \approx 0\overset{m}{.}4$ using the measured equivalent width of the interstellar band W(5780)≈0.2 Å and correlation W(5780)–E(B-V) from [17].

  Even with $Mv \approx -4^m$ (such a luminosity would rather correspond to a star from the upper part of the main sequence than to a supergiant), d≈ 4 kpc. It is the lower limit of the MWC 17 distance. However, the estimates of both the stars color and its spectral type are unreliable until the distorting influence of emissions is taken into account and photospheric lines are detected. However, if we bear in mind that according to Miroshnichenko [18], the visual magnitude of the star $V \approx 13^m$, then the distance to it will be considerably greater.

– According to [19], the interstellar extinction toward MWC 17 reaches $2\overset{m}{.}5$ at a distance of 1 kpc and remains almost the same up to 3–4 kpc. If we assume the above estimated Av$\approx 2\overset{m}{.}5$ for MWC 17, we will obtain only a limitation on the objects distance, d>1 kpc.

– Among the velocities given in Table 4, the closest to Vsys can be the velocities of the forbidden emissions: −47 km/s (Vlsr =−42 km/s). By Brand and Blitz [20], a distance d≥2 kpc corresponds to this value.

There is an important additional point: in the sky, MWC 17 is located at the southern boundary of the compact association Cas OB 8 (d≈2.9 kpc from [21]). For the member of this association HD 9311, Vr =−42 km/s; the structure of the interstellar NaI lines in its spectrum is similar to that in the MWC 17 spectrum (Vr≈ −(65 ÷ 50), −14 km/s [22]). Obviously, the question on possible membership of MWC 17 in Cas OB 8 is a key one for determination of the distance and origin of the object. Meanwhile, we have to assume that the distance to MWC 17 can be of the order of both 4–5 kpc and 2–3 kpc — in the case there is some additional (possibly circumstellar) extinction.

The profile of the NaI D lines in the MWC 17 spectrum is close to that observed in the spectrum of the hot B-type star – the optical component of the IR-source IRAS 00470+6429, which is located near the galactic plane and has the coordinates $\alpha(2000) = 00^h\,50^m\,06^s$, $\delta(2000) = +64^\circ\,45'\,35''$, $l = 122\overset{\circ}{.}8$, and $b = 1\overset{\circ}{.}9$. In the optical spectrum of its central star, there are two interstellar components of the NaI D lines [7]. Heliocentric radial velocities in the IRAS 00470+6429 spectrum (about −62 and −13 km/s) coincide with those in the MWC 17 spectrum. In the spectra of both objects, the positions of diffuse interstellar bands are also similar: Vr(DIB)≈ −14 km/s.

5. Conclusions

High quality of the spectral data which we used allowed us to identify numerous details in the spectrum of MWC 17. The thorough search has not led to detection of any absorptions in the spectrum which emerge in the stellar atmosphere. Out of absorption details, only interstellar components of the NaI D lines and DIBs were identified. The DIBs are weak, the equivalent widths are W(5780)≈ 0.2 Å and W(5797)≈ 0.15 Å.

As a systemic velocity, Vsys, the velocity for forbidden emissions can be accepted: −47 km/s (relative to the local standard Vlsr =−42 km/s).

Comparison between our results and the measurements of Zickgraf [8] allows us to draw an inference on the absence of significant variability of spectral details.

We noticed variations of radial velocities from spectrum to spectrum which are small and can hardly give sure evidence on spectral binarity of MWC 17. In order to solve this problem, observations of this star with high positional accuracy should be continued. Taking into account high intensity of the emission details in the spectrum of this faint star, such observations can be also made on telescopes of a moderate diameter.

Acknowledgements

The authors are grateful to V.E. Panchuk and M.V. Yushkin for considerable assistance with the observations on the BTA. The study was fulfilled with the financial support of the Russian Foundation for Basic Research (project 14–02–00291 a). The observations on the 6-m telescope of the Special Astrophysical Observatory was conducted with the support of the Ministry of Education and Science of the Russian Federation (agreement No. 14.619.21.0004, project ID RFMEFI61914X0004). The astronomical databases SIMBAD and ADS were used in the study.

REFERENCES

1. D.A. Allen and J.P. Swings, Astron. & Astrophys. **47** 293 (1976).
2. P.S. The, D. de Winter, & M.R. Perez, Astron. & Astrophys. Suppl. **104** 315 (1994).
3. H.J.G.L.M. Lamers, F.J. Zickgraf, D. de Winter, et al., Astron. & Astrophys. **340** 117 (1998).
4. A.S. Miroshnichenko, Astrophys. J. **667** 497 (2007).
5. M. Kraus, M. Borges Fernandes, & O. Chesneau, ASP Conf. Ser. **435** 395 (2010).
6. D.M. Kelly & B.J. Hrivnak, Astrophys. J. **269** 1040 (2005).
7. A.S. Miroshnichenko, E.L. Chentsov, V.G. Klochkova, et al., Astrophys. J. **700** 209 (2009).
8. F.–J. Zickgraf, Astron. & Astrophys. **408** 257 (2003).
9. V. Panchuk, V. Klochkova, M. Yushkin, & I. Najdenov, J. Optical Technology **76** 87 (2009).
10. V.E. Panchuk, M.V. Yushkin, & I.D. Najdenov, Preprint No. 179 (Special Astrophysical Observatory, Nizhny Arkhyz, 2003).
11. M.V. Yushkin & V.G. Klochkova, Preprint No. 206 (Special Astrophysical Observatory, Nizhny Arkhyz, 2005).
12. V.G. Klochkova, V.E. Panchuk, M.V. Yushkin, & D.S. Nasonov, Astrophysical Bulletin **63** 386 (2008).
13. P.W. Merrill & C.G. Burwell, Astrophys. J. **78** 87 (1933).
14. C.S. Beals, Publ. Dominion Astrophys. Obs. **9** 1 (1953).
15. C. Jaschek & Y. Andrillat, Astron. & Astrophys. Suppl. **136** 53, (1999).
16. M.T. Martel and R. Gravina, IBVS, No. 2750 (1985).
17. S.D. Friedman, D.G. York, B.J. McCall, et al., Astrophys. J. **727** 33 (2011).
18. A.S. Miroshnichenko, private communication.
19. Th. Neckel, G. Klare, & M. Sarcander, Astron. & Astrophys. Suppl. **42** 251 (1980).
20. J. Brand & L. Blitz, Astron. & Astrophys. **275** 67 (1993).
21. R.M. Humphreys, Astrophys. J. Suppl. **38** 309 (1978).
22. G. Münch, Astrophys. J. **125** 42 (1957).

Table 5: Central residual intensities and heliocentric radial velocities for the lines in the MWC 17 spectrum. Designations are the same as in Table 2. Uncertain measurements are marked with a colon

Ident	λ	r	Vr	V_{em}		V_{abs}	V(r/2		V(r≈1)	
[SII]1F	4068.60	4.6	−48:				−77:	−22:	−98:	−5:
[SII]1F	4076.35	2.7:	−47:							
Hδ	4101.74	5.9			−23	−61:				
FeII(28)	4178.85	2.7	−48	−67:	−24:	−46	−90:	−7:	−100:	7:
FeII(27)	4233.17	4.8	−50	−68:	−35	−49	−84:	−21:	−105:	10
[FeII]21F	4243.98	2.6:	−47:							
[FeII]21F	4276.83	3.1:	−50							
[FeII]7F	4287.39	7.1	−48	−57	−42	−52	−72:	−26:	−95:	5:
[FeII]21F	4319.62	2.1	−48:							
Hγ	4340.47	14.0			−21:	−58				
[FeII]7F	4359.33	5.6	−46					−25:		0:
FeII(32)	4413.59									
[FeII]7F	4413.78	4.6	−50				−74:	−27:	−111:	−3:
[FeII]6F	4416.27	4.3								
[FeII]7F	4452.10	3.4	−48	−57:	−40	−50:	−74:	−26:	−98:	−4:
[FeII]6F	4457.94	2.6	−47	−60:	−40:	−52:	−74:	−28:	−102:	−7:
HeI(14)	4471.52	2.3	−48:	−82:	−29:	−59:	−105:		−142:	
[FeII]7F	4474.90	2.4	−49:				−80:	−22:	−108:	−3:
FeII(37)	4491.40	2.0:	−53:	−73:	−31:	−52:	−92:		−105:	
FeII(38)	4508.28	2.0	−50	−72:	−37	−51:			−92:	8:
FeII(37)	4515.33	3.4	−51	−67	−28:	−49:	−87:	−18:		
FeII(37)	4520.22	3.4	−50	−69:	−27:	−45:	−89:	−8:	−106:	
FeII(38)	4522.63	3.4	−51	−65	−33:	−49:	−81:	−19:	−102:	7
FeII(38)	4549.47	3.1	−51	−70:	−32:	−50:	−87:	−15:	−107:	0:
TiII(82)	4549.63									
FeII(37)	4555.89	3.6	−50	−72:	−30	−45	−89:	−13:	−107:	2:
FeII(38)	4576.33	2.1	−50:							
FeII(38)	4583.83	6.5	−49	−70	−35	−51:	−87	−10		13:
FeII(37)	4629.33	6.0	−50	−71	−35:	−51:	−88	−10:	−109:	12:
[FeII]4F	4639.67	2.5	−49:		−47:		−75:	−28:	−90:	−10:
[FeIII]3F	4658.1	7.0	−46	−67:	−21	−49 :	−91:	−7:	−122:	16
FeII(37)	4666.75	2.0	−49:	−68:	−22:				−123:	3:
[FeIII]3F	4701.5	2.6:	−46:	−68:	−17:	−45:	−92:	−4:	−108:	14:
HeI(12)	4713.18	1.5:	−49:	−88 :	−20:	−52:				
[FeII]4F	4728.07	4.0:	−46	−53 :	−42:	−48:	−69:	−26:	−94:	0:
FeII(43)	4731.47	1.7:	−51:						−95:	−4:
[FeIII]3F	4733.9	1.8:	−48:	−60 :	−24:	−42:				
[FeIII]3F	4754.7	2.0	−48:	−75 :	−23:	−55:			−112:	20:
[FeIII]3F	4769.4	1.7:	−43:	−63 :	−18:	−44:			−95:	10:
[FeII]20F	4774.72	2.2	−48				−69:	−25:	−94:	−8:
[FeIII]3F	4777.7	1.3:	−51:	−65 :	−23:	−42:			−114:	23:
[FeII]20F	4814.53	4.8:	−46	−56 :	−42:	−52:	−75:	−24:	−102:	5:
CrII(30)	4824.14	1.3:	−46:	−69 :	−23:	−50:			−104:	9:
Hβ	4861.33	12.0:				−96:				
					−15	−56				

Table 5, to be continued

Ident	λ, Å	r	Vr	V_{em}		V_{abs}	V(r/2)		V(r≈1)	
[FeII]20F	4874.48	2.1	−47				−74:	−24:	−90:	0:
[FeII]4F	4889.62	4.8	−47	−54:	−42:	−50:	−70:	−26:	−98:	−1:
[FeII]	4898.61	2.2	−48						−90:	−16:
[FeII]20F	4905 34	3.0	−47	−53:	−41:	−49:	−73:	−23:	−98:	0:
HeI(48)	4921.93	2.1:	−51:	−101:	−25:				−115:	
FeII(42)	4923.92	6.0	−43:	−55	−36	−50	−75	−17	−103:	8:
[FeIII]1F	4930.5	1.7	−42:	−69:	−18:	−55:	−83:	5:	−106	25:
[FeII]20F	4947.37	1.8	−45:						−80:	
[FeII]20F	4950.74	1.9	−45				−64:	−27	−83:	−8:
[OIII]1F	4958.92	2.0	−48:				−127:	21:	−170:	90:
[FeII]20F	4973.39	2.1	−48	−58:	−40:	−47:	−70:	−26	−90:	−8:
[OIII]1F	5006.84	4.0	−56:	−100:	−50:	−78:	−130:	19:	−183:	95:
[FeIII]1F	5011.3	2.5	−46	−60:	−22	−48:	−92:	−9:	−119:	20:
HeI(4)	5015.68	3.6	−47:	−73:	−23	−46:		−2:	−120:	20:
FeII(42)	5018.44	6.5	−43	−55	−37	−51:	−72:	−20	−108:	6:
[FeII]20F	5020.23	2.0:	−45:		−40:	−46:				
FeII	5030.64	1.8:	−45:	−62:	−37	−53:	−70:	−22:	−93:	−5:
SiII(5)	5041.03	2.1	−46				−78:	−18:	−110:	2:
[FeII]20F	5043.52	1.6	−46						−85:	−11:
HeI(47)	5047.74									
[TiII]19F	5047.91	2.0	−45:							
SiII(5)	5056.06	2.8	−46		−36:	−49:	−95:	−5:	−130:	20:
[FeII]	5060.08	1.5	−47				−72:	−27:	−82:	−18:
FeII	5070.90	1.5	−48:							
[FeII]19F	5072.39	1.3:	−47:							
FeII	5075.77	1.3:	−43:							
FeII	5089.22	1.5	−48:	−68:	−42:	−51:	−83:	−17:	−98:	0:
FeII	5100.74	1.3	−46:				−86:	−23:	−105:	−4:
[FeII]18F	5107.94	1.7	−49				−80:	−28:	−96:	−12:
[FeII]19F	5111.63	2.0	−47	−61:	−42		−75:	−22:	−92:	−7:
FeIII(5)	5114.10	1.7	−44							
FeIII	5149.33									
FeII	5149.46	1.5								
[FeII]18F	5158.00									
[FeII]19F	5158.78	5.5	−50	−55:	−42:	−48:	−102:	−21		4:
[FeII]35F	5163.95	2.4	−46	−53:	−40:	−49:	−68	−26	−85:	−4:
FeII(42)	5169.03	6.0	−42	−55	−36	−50:	−70:	−17	−100:	7:
[FeII]18F	5181.95	1.9	−46				−72:	−28:	−90:	−10:
FeII(49)	5197.58	4.0	−50	−72	−33	−52:	−89	−10:	−109:	3:
[FeII]35F	5199.17	1.9	−48:					−23:		−4:
FeII	5203.64	1.4	−47		−45:	−58:	−78:	−16:	−90:	−4:
FeII	5216.85	1.8	−45:				−74:	−19:		−5:
[FeII]19F	5220.06	2.1	−46	−53:	−41:	−48:	−71:	−24:	−93:	−6:
FeII(49)	5234.62	4.2	−50	−71	−33	−52:	−90	−9	−106:	10:
FeII	5247.95	1.4	−47:				−84:	−13:	−97:	13:
FeII	5251.23	1.2	−47:						−96:	0:
FeII(49)	5254.93	1.5:	−54:	−72:	−31:	−50:			−114:	−4:
[FeII]19F	5261.62	4.5	−46	−54	−42	−50:	−74:	−22:	−99:	8:
FeII	5264.18									
MgII917)	5264.22	2.0	−45:							

Table 5, to be continued

Ident	λ, Å	r	Vr	V_{em}		V_{abs}	V(r/2)		V(r≈1)	
FeII(48)	5264.80									
[FeII]18F	5268.87	2.4	−46:							
[FeIII]1F	5270.40	4.3	−42	−62:	−15	−45:		−4		18:
[FeII]18F	5273.35	4.9	−47	−52:	−41:	−50:	−70	−27	−98:	0:
FeII(49)	5276.00	6.5	−50	−70	−32:	−47:	−88	−10	−112:	9:
FeII(41)	5284.10	4.0								
FeII	5291.67	1.9	−47	−60:	−33:	−51:	−78:	−15:	−100:	2:
[FeII]19F	5296.83	2.0	−47				−74	−26:	−92:	−10:
FeII(49,48)	5316.66	2.0	−51	−69	−35	−51	−88	−13	−114:	13:
FeII(49)	5325.56	1.8	−50	−75:	−33:		−90:	−3:	−103:	3:
OI(12)	5330.74	1.4	−49:							
[FeII]19F	5333.65	4.0	−47		−42:		−72	−25	−95	0:
FeII(48)	5362.87	3.0	−51	−73	−35:	−48:	−91	−10:	−108:	8:
[FeII]19F	5376.45	3.6	−47	−54:	−42	−51:	−71	−27	−100:	−2:
FeII	5402.06	1.5	−43:				−73:	−20	−100:	5:
[FeII]17F	5412.65	2.3	−49	−54:	−44:	−49:	−77:	−26	−105:	−2:
FeII(48)	5414.05									
FeII(49)	5425.25	2.1	−51	−73:			−91	−10	−106:	10
FeII	5427.82	1.2	−52:							
FeII(55)	5432.98	2.5:								
[FeII]18F	5433.13	1.7:	−48:							
FeII	5457.72	1.4	−47				−75:	−21:	−89:	−3:
[FeII]	5477.24	1.8	−47				−71:	−25:	−83:	−17:
FeII	5482.31	1.5	−51:	−78:	−34:		−87:	−18:	−98:	−5:
FeII	5487.63	1.3	−50:							
[FeII]17F	5495.82	1.5	−46				−69:	−21:	−80:	−4:
[FeII]17F	5527.34	3.3	−47	−53:	−42:	−50:	−72	−24	−92:	−6:
FeII(55)	5534.83	4.0	−50	−75	−35:	−45:	−90	−9	−106:	10:
[FeII]39F	5551.31	1.4	−45				−69:		−85:	
OI(24)	5554.95	1.4	−46:							
[OI]3F	5577.34	2.3	−45	−69:	−33:	−51:	−85:	−4:	−98:	10:
[FeII]39F	5588.15	1.4	−47:						−98:	−3:
[FeII]	5613.27	1.3	−47:							
[FeII]	5673.21	1.6	−47	−55:	−40:	−49:	−75:	−26		−10:
[FeII]17F	5745.70									
[FeII]34F	5746.97	2.6	−47	−54:	−41:			−28		−5:
[NII]3F	5754.64	17.0	−47	−65	−32	−53	−84	−15	−122:	8:
FeII	5780.12	1.4:	−48:							
DIB	5780.37	0.7	5:							
FeII	5783.63	1.4	−46:							
DIB	5796.96	0.8	−8:							
FeII(58)	5835.49	1.7	−51:							
HeI(11)	5875.72	7.5	−52	−75:	−28	−54:	−106:	−7:	−145:	28:
FeII	5885.02	1.3:	−41:							
NaI(1)	5889.95	0.6	−59:							
		0.2	−50							
		0.3	−38							
		0.1	−27							
		0.1	−10							
NaI(1)	5895.92	0.7	−60:							

Table 5, to be continued

Ident	λ, Å	r	Vr	V_{em}		V_{abs}	V(r/2)		V(r≈1)	
		0.3	−50							
		0.4	−40							
		0.1	−27							
		0.1	−9							
[FeII]34F	5901.26	1.2:	−42:							
FeII	5902.83	1.4	−48:	−74:	−36:				−89:	−9:
SiII(4)	5957.56	3.3								
OI(23)	5958.6									
FeII	5965.63	1.2	−47:							
SiII(4)	5978.93	4.3	−47:	−57:	−37:	−51:	−86:	−15	−118:	10:
OI(22)	6046.4	4.2								
FeII(46)	6113.32	1.2	−47:							
CaI(3)	6122.22									
MnII(13)	6122.44	1.3	−46:							
MnII(13)	6122.80									
MnII(13)	6123.16									
[TiII]22F	6124.57									
SiI(30)	6125.02	1.9								
FeII(74)	6147.74	1.4								
FeII(74)	6149.25									
OI(10)	6155.98									
OI(10)	6156.77									
OI(10)	6158.18	1.4	: −50:							
[FeII]44F	6188.55	1.3	: −47:							
DIB	6195.96	0.8	−12:							
FeII	6233.53	2.1	−50				−88:	−14:	−100:	9:
FeII(74)	6238.39	1.5:	−50:							
FeII(74)	6239.90									
FeII(74)	6247.55	2.0:								
FeII	6248.89	3.7								−13
DIB	6283.85	0.8								
FeII	6291.83	1.7	−49:				−85:	−12:	−100:	6:
[OI]1F	6300.30	30.0	−48	−58	−39	−50	−74	−23	−93	−2
[SIII]3F	6312.10	4.6	−48:	−62:	−49:	−26:	−80:	−12:	−118:	5:
FeII	6317.99	8.8	−50	−61:	−36	−50:	−87	−14	−105:	8:
SiII(2)	6347.10	4.5	−47	−56:	−38:	−51:	−88	−15	−120:	15:
FeII	6357.17	1.3	−52:							
[OI]1F	6363.78	12.0	−48	−58	−39	−49	−74	−24	−93:	−5:
FeII(40)	6369.46									
SiII(2)	6371.36	3.0	−47				−84:	−18:	−120:	5:
FeII	6375.79	1.2	−49						−90:	−5:
FeII	6383.72	5.1	−51	−62:	−37:	−49	−86:		−105:	
FeII	6385.45	3.3	−48:	−64:	−34:	−47:		−16		7:
FeII(74)	6416.92	1.6	−52:	−74	−28:	−42:	−87:		−102:	0:
FeII(40)	6432.68	1.5	−52:						−115:	10:
FeII	6442.95	2.6	−50	−60:	−35 :	48	−86:	−12:	−100:	3:
FeII	6455.84	3.5								
FeII(74)	6456.38	2.6								
FeII	6491.25	2.1	−49:				−84:		−99:	
FeII	6493.03	2.6	−51					−14:		5:

Table 5, to be continued

Ident	λ, Å	r	Vr	V_{em}		V_{abs}	V(r/2)		V(r≈1)	
[NII]1F	6548.03	1.5	−47				−85:	−13:	−115:	10:
Hα	6562.81		−52:		−12	−108:				
						−54				
[NII]1F	6583.45	3.4	−46				−82	−10	−115:	15:
FeII	6586.70	1.3	−50:				−86:	−12:	−102:	7:
DIB	6613.56	0.8	−19:							
HeI(46)	6678.15	2.5	−53	−72:	−26	−60:	−105:	−1:	−135:	20:
[SII]2F	6716.47	1.5	−48				−65:	−27:	−80:	−15:
[SII]2F	6730.85	2.0	−48				−71:	−26:	−95:	−5: